JETIR.ORG ISSN: 2349-5162 | ESTD Year : 2014 | Monthly Issue
JOURNAL OF EMERGING TECHNOLOGIES AND INNOVATIVE RESEARCH (JETIR)
An International Scholarly Open Access, Peer-reviewed, Refereed Journal

Field relationship and Geochemical characterization of Amphibolites from Khammam schist belt at the margin of the Eastern Dharwar Craton, South of Wyra, Khammam District, Telangana, South India

[1]Venkanna Banothu and [2]Dr. Linda Prabhakar Babu
[1]SU: Telangana, Southern Region, Geological Survey of India and Osmania University, Hyderabad, India-500068
[2]Osmania University, Hyderabad, India-500007
Email: venkannageologist@gmail.com

Abstract:

The Archaean schist belts are remnants of once larger tracts of meta-volcanic and meta-sedimentary rocks that are mostly metamorphosed from greenschist to amphibolite facies. Amphibolite belonging to the Khammam Schist Belt (KSB) marked at the eastern fringe of the Eastern Dharwar Craton (EDC) still retains its parental basic magmatic signatures in terms of lithological association, mineral assemblage and geochemical character, which provides a clear picture of the Archaean magmatic activity, their petrogenesis and mode of evolution. Amphibolites occur as sporadic enclaves within the granite gneiss of Peninsular Gneissic Complex (PGC-II) exhibits strong foliation with epidote-amphibolite facies metamorphic mineral assemblages. Amphibolites of KSB from the Wyra area contains lower ferromagnesian values and low Ni (<200 ppm) content suggests fractionation of magma. Most of the amphibolites are having basaltic to basaltic-andesite composition classified as tholeiitic magmatic series indicating strong enrichment of iron in the initial stages. The high enrichment of LILE, LREE and depletion of HREE with pronounce negative troughs of Nb and Ti in the amphibolite is the product of volcanic arc basalt.

Keywords: Khammam schist belt, Eastern Dharwar Craton, Eastern Ghats Belt, Amphibolites

1. INTRODUCTION:

The eastern margin of the Eastern Dharwar Craton is an ideal terrain segment to evaluate the crustal evolution in terms of granulite-granite and greenstone- granite relations, formation of a sedimentary basin at the craton- mobile belt junction, and the extensional tectonics leading to the formation of Godavari graben (Fig.1). This segment exposes the litho-units constituting the granite complex of Dharwar craton in particular Eastern Dharwar Craton, Shernawala outlier of Pakhal Supergroup, granulites of Eastern Ghats Belt. The Marginal Zone intervening the craton and mobile belt, and outliers of Gondwana sediments, all intricately welded together (Sarvothaman, 1996). Besides, a transcratonic supracrustal belt namely Khammam Schist Belt and the Chimalpahad Anorthosite Complex occur in the Marginal Zone (Fig.2). The study area is a junction of craton (EDC: Eastern Dharwar Craton), mobile belt (EGB: Eastern Ghats Belt) and granite-greenstone belt (KSB: Khammam Schist Belt) where the rocks of the EDC is having the ensembles of KSB and EGB rocks. Generally, the craton and mobile belts contacts are defined by the terrane boundary shear/suture/thrust zones which play a vital role in the amalgamation of two different tectonic domains. The western boundary of the EGB is defined by

the Eastern Ghats Boundary Fault/thrust along the northern part of EGB with Singhbhum and Bastar Craton whereas, the southern part of the EGB shares the boundary between EDC with EGB is ambiguously defined. Interestingly, the study area is the ideal geographic location particularly, T.S. 65C/8 (southern part) where EDC group of rocks are having direct contact with EGB. However, the EGB group of rocks shares the tectonic contact with Nellore Schist Belt and farther west Cuddapah Basin does not relay any direct contact. The grade of metamorphism in the KSB generally increases from greenschist to upper amphibolite facies from west to east (Vasudevan and Rao, 1985; Ramam and Murty, 1997; Babu, 1998; Moeen, 1998). Sarvothaman (1995) reported the presence of kyanite-garnet assemblage P-T regime between 650 - 750ºC and 0.8- 1.2 ±0.2 Gpa from garnetiferous amphibolites within the KSB is also reported (Kumar et al., 2000; Hari Prasad et al., 2000; Okudaira et al. 2001). The Sm-Nd and Rb-Sr isochron ages of garnet-clinopyroxene amphibolite from the KSB is reported to be having a protolith age of 3.37-3.62 Ga and were tectonically reworked at 0.824±0.043 Ga during the high-pressure metamorphic condition and having 0.481±0.016 Ga Pan-African thermal imprint (Okudaira et al., 2001).

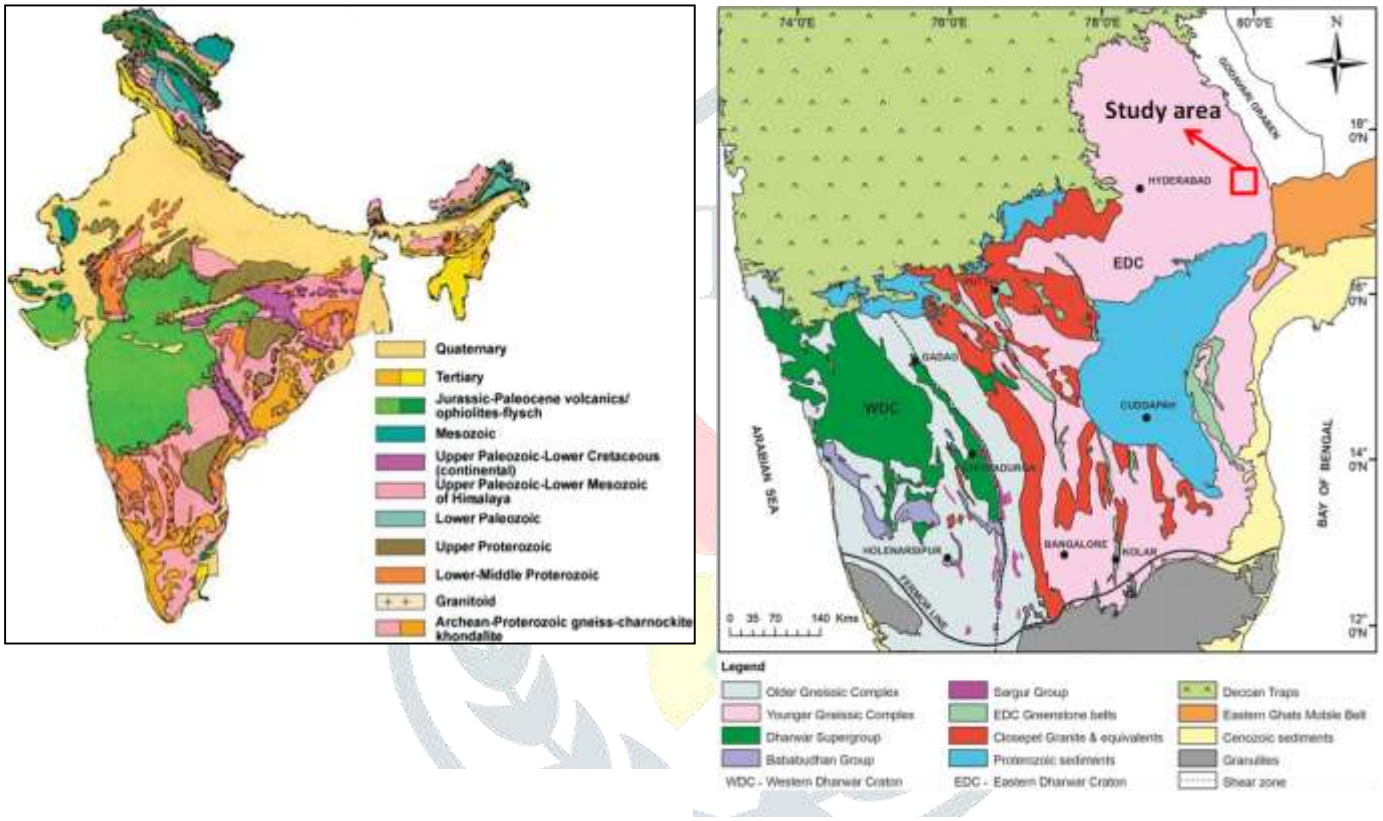

Figure 1: Generalized geological map of the India showing Dharwar Craton, Southern India (after Geological Survey of India, 1996).

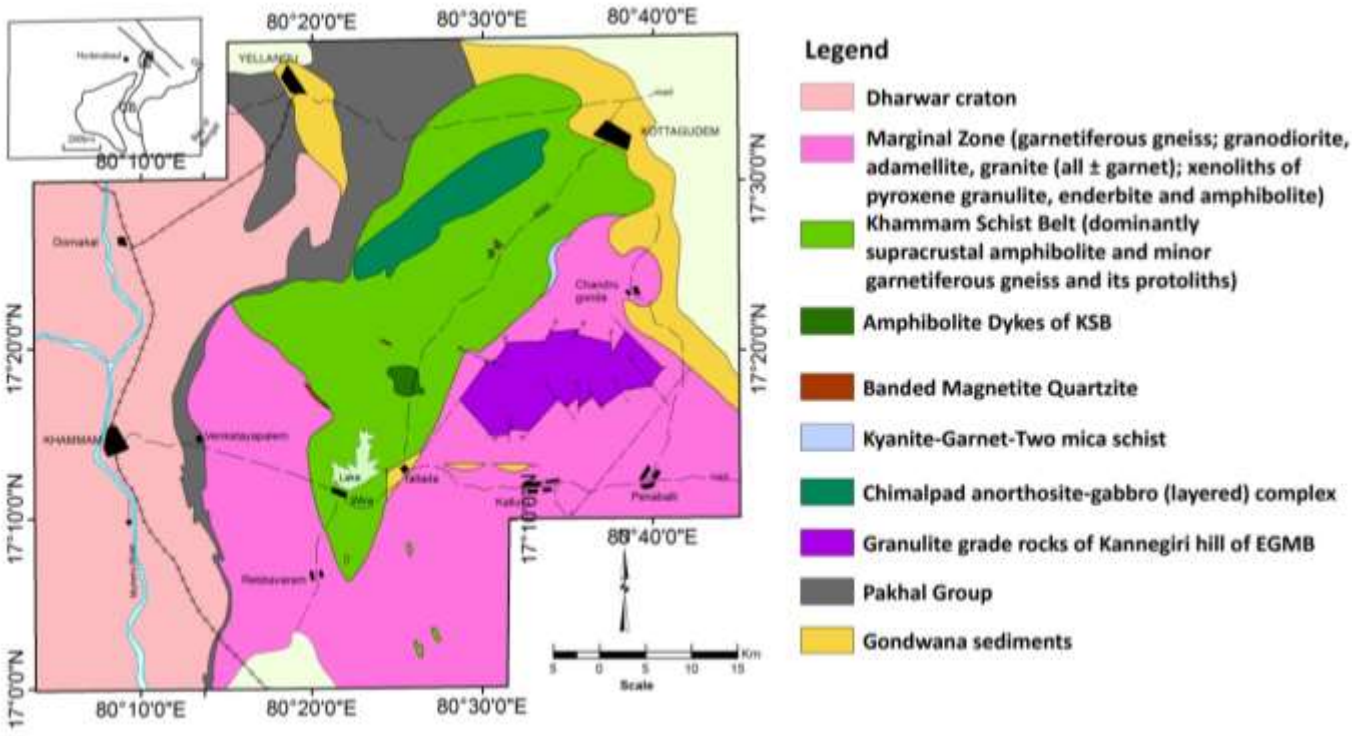

Figure 2: Generalized geological map of the Dharwar Craton, Southern India (after Sarvothaman, 1996).

2. GEOLOGICAL SETUP:

Generally, most of the schist belts in EDC form as a linear trend (Gadwal schist belt, Paddavuru schist belt, Ghanpur schist belt and Yerraballi schist belt), whereas the Khammam Schist Belt (KSB) rocks occur as sporadic outcrops within the granite gneisses of Peninsular Gneissic Complex (PGC-II) in the eastern flank of EDC (Fig.3). The presence of Archaean equivalent rocks is firmly reported by Appavadhanulu, 1961; Kumar and Somayajulu, 1981, which are represented by garnet-biotite schists, quartz-biotite schists, garnet-kyanite-muscovite schists, calc-silicate rocks, banded iron formations, quartzites, hornblende schists and gneisses. The KSB largely comprised of meta-basics and minor meta-sedimentary rocks which is correlated to Sargur Supergroup by Subbaraju (1975) and the transcratonic supracrustal belt by Sarvothaman (1996). Sarvothaman (1996), differentiated the existence of two varieties of amphibolite in the area i.e., i) supracrustal amphibolite and ii) amphibolite dykes, based on field relationship, petrographic study and geochemical signatures. Surya Prakash Rao et al (1990) have indicated that these amphibolites are meta-igneous rocks. A meta-basic volcanic suite, comprising hornblende schist, hornblende gneiss and amphibolite is the most dominant constituent of the supracrustal belt. Some of these rocks are garnetiferous and clinopyroxene bearing (Hari Prasad et al., 2000; Sarvothaman, 1995). Talc-tremolite-actinolite schists, representing metamorphosed ultramafic intrusions, occur as scattered conformable lenses. The rock of the PGC-II predominantly comprises grey hornblende biotite granite gneiss, porphyritic alkali feldspar granite, and intrusives of dolerite dykes with enclaves of Khammam schist belt rocks. The Kannegiri granulite includes garnet-sillimanite gneiss, quartzite, calc-granulite and pyroxene granulite confined in the eastern part. A curvilinear sequence of dolomite, phyllite and quartzite bands belonging to the Pakhal Supergroup trends almost N-S trend in the western part.

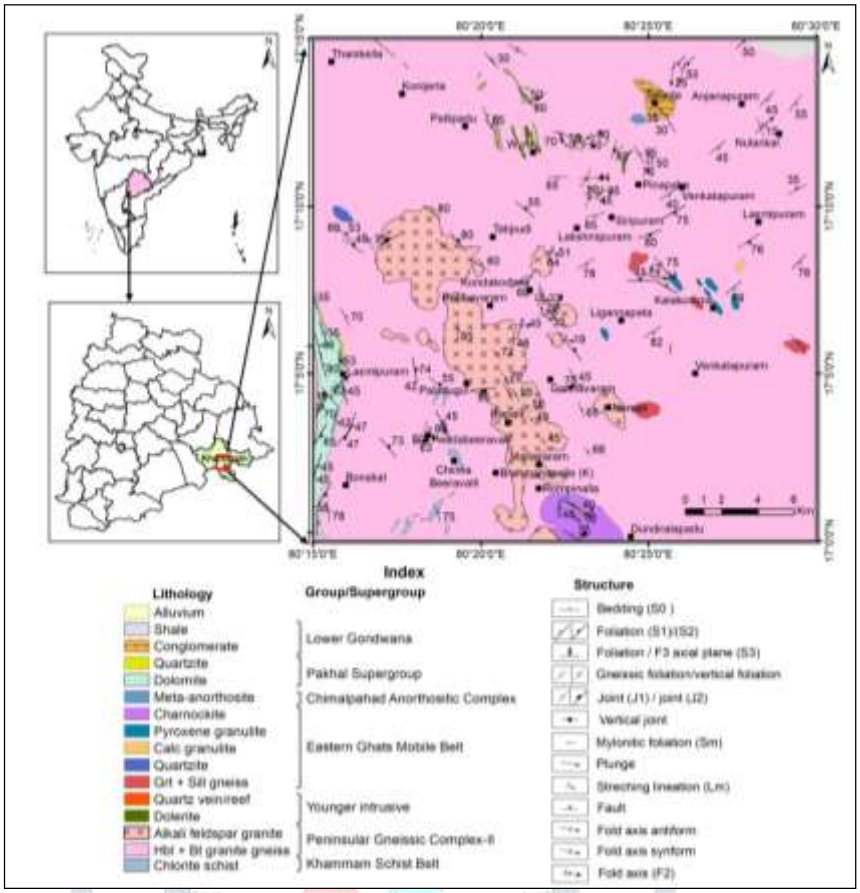

Figure 3. Generalized geological map showing the various lithologies made up of PGC-II of Archaean to Palaeoproterozoic age, Khammam schist of Archaean, Eastern Ghats Supergroup of Archaean to Proterozoic age and Pakhal Supergroup of Mesoproterozoic age and Gondwana Supergroup of Carboniferous to Lower Triassic age (modified after GSI, A.K Reddy, 1976, K.N Srinivasan 1986 and S.T. Narahari, 2002).

3. FIELD RELATIONS:

Among all litho-units of KSB, the amphibolite is the dominant rock type marked between the Shernavala outlier in the west and Kannegiri granulites in the east. Amphibolites bands found as small enclaves within the granite gneisses of PGC-II towards the south of Wyra, Khammam District, Telangana. For field relationship and geochemical study, the two type localities were identified and mapped in detail i.e., a) amphibolite from Kalakodima in the eastern part and b) amphibolite from Paladugu in the western part (Fig.4a). Amphibolite from the eastern part is medium to coarse-grained, occasionally contains garnet occurs both massive as well as foliated variants within the country-rock of garnetiferous biotite granite gneiss (Fig.4b). Whereas, amphibolite bands in the western part are associated with quartz chlorite schist and quartzite within the country-rock of hornblende biotite granite gneiss (Fig.4c). Megascopically, these amphibolites show fine-grained texture, dark greenish colour and are strongly foliated (Fig.5a). Foliation represented by parallel alignment greenish amphiboles/pyroxene and elongated feldspars (Fig.5b). At places, the amphibolites are associated with a linear sequence of banded grunerite quartzite, banded magnetite quartzite, ferruginous quartzite (Fig.5c). At outcrop scale, these foliation planes are folded to produce mesoscopic tight to open vertical folds (Fig.5d). Within the granite gneiss, the small patches of amphibolite bands observed are also oriented parallel to the gneissic foliation (Fig.5e).

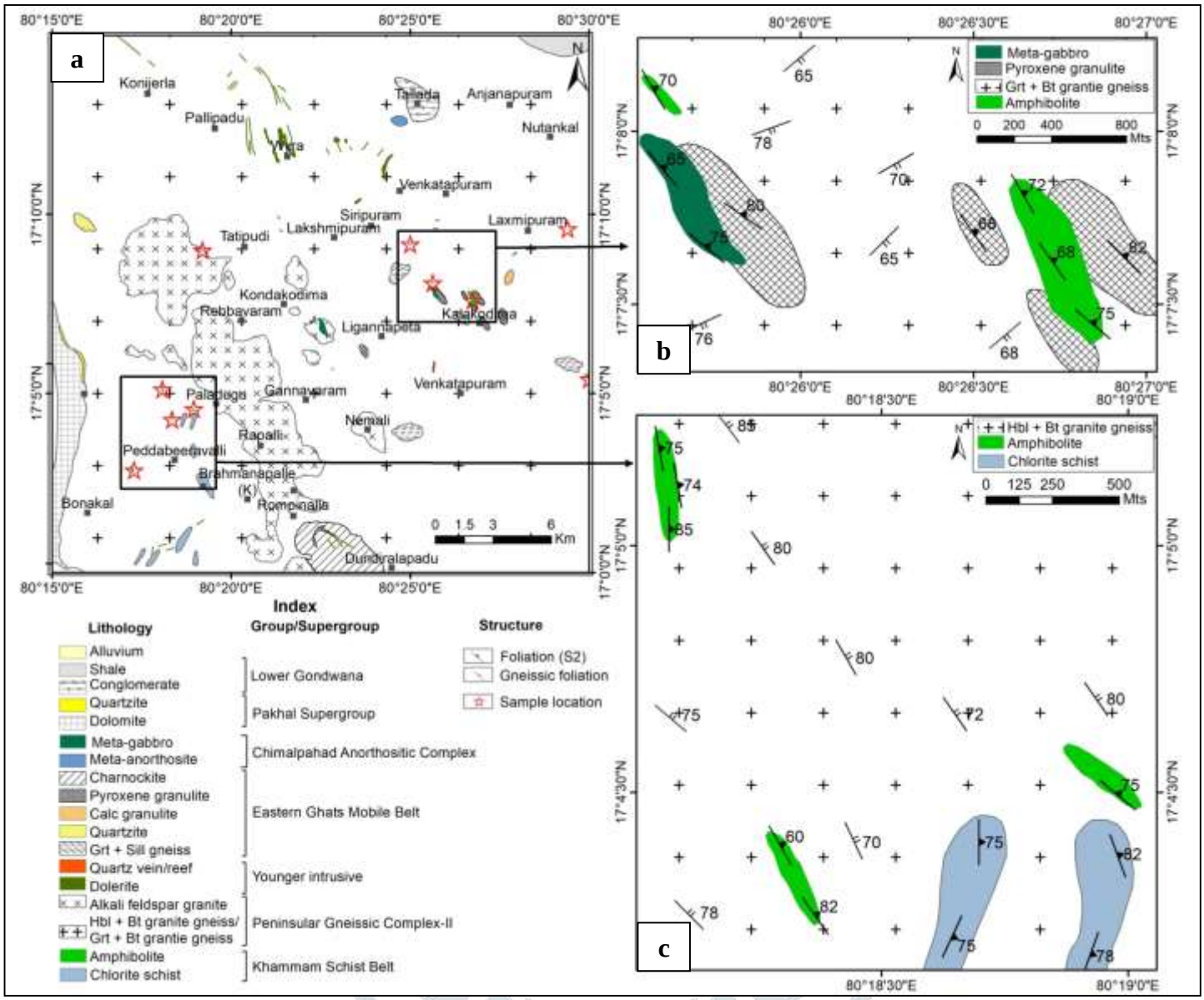

Figure 4 (a). Geological map around Wyra, Khammam District, showing the study area with cluster of amphibolite and sample locations (modified after GSI). (b) Amphibolite from Kalakodima area (c) Amphibolite from Paladugu area.

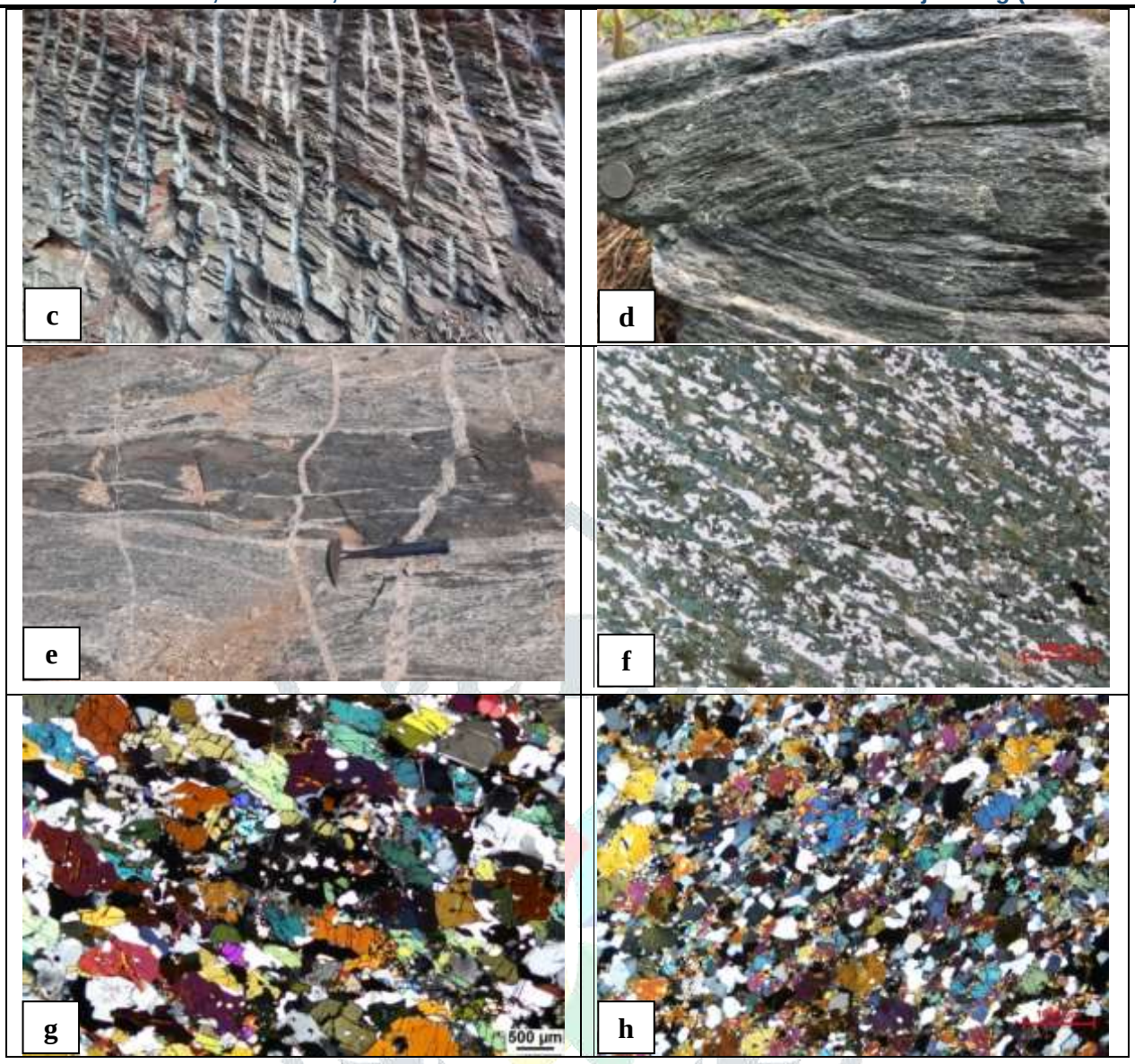

Figure 5 (a). Field Photograph of amphibolite exposure from Paladugu area. (b) Foliated amphibolite. (c) Strongly foliated amphibolite associated with quartz-grunerite schist. (d) Outcrop scale mesoscopic fold in amphibolite. (e) Amphibolite enclave within the hornblende biotite granite gneiss. (f) Photomicrograph of amphibolite exhibiting the preferably alignment of amphiboles and feldspar segregation. (g) Garnetiferous amphibolite with relict clinopyroxene grains partially transformed to hornblende. (h) Amphibolite showing nematoblastic texture comprises of plagioclase, amphibole ± epidote ± quartz.

4. PETROGRAPHY:

Under the microscope, amphibolite from the western part (Paladugu area) exhibits preferential and parallel alignment of prismatic amphiboles and fine-grained elongated feldspar segregation clearly illustrates the strong schistosity (Fig. 5f). The hornblende grains occur both as a cluster of relatively larger subhedral grains and smaller greenish prismatic grains within the feldspathic groundmass. The smaller prismatic hornblende grains show preferred orientation defining the foliation planes, sometimes forming alternate bands of hornblende and feldspar. The garnetiferous amphibolites from the eastern part (Kalakodima area) are predominantly composed of medium to coarse-grained hornblende with relict clinopyroxene, plagioclase and accessory minerals like epidote with a minor amount of small magnetite grains. Garnet mostly occurs as porphyroblastic nature with inclusions of quartz and amphibole (Fig. 5g). The development of strong nematoblastic texture is represented by the preferred alignment of hornblende grains and elongated/epidote aggregates parallel to the foliation planes (Fig. 5h).

5. GEOCHEMISTRY:

Bulk geochemical analysis for 10 nos. amphibolites samples for major and trace elements (Table 1) by X-ray Fluorescence (XRF) spectrometry using a 4KW Rhodium anode tube, whereas REEs (Table 2) by LA-ICP-MS (Laser Ablation-Inductively Coupled Plasma-Mass Spectrometry) using a CETAC Nd: YAG 213nm, Laser Ablation (LA) system coupled with Agilent 7700x., at the Chemical Division, Southern Region, Geological Survey of India, Hyderabad. The major element distribution of oxides in amphibolites has moderate SiO_2 wt% from 47.76 to 52.06% and averages 50.20%. Al_2O_3 wt% widely varies from 6.25 to 13.78% and averages 10.81%. The concentration of MgO wt% ranges between 4.64 to 12.60% and averages at 7.48%. Iron oxide in the form of total Fe_2O_3 wt% concentration also varies from 8.36 to16.77% and averages at 13.16%. The CaO wt% lies between 9.75 to 13.21% and averages at 10.73%. In term of alkalies, both the Na_2O wt% as well as K_2O wt% low values lies between 1.01 to 3.53% and 0.31 to 1.67% respectively. P_2O_5 shows a limited range of distribution ranging between 0.12 to0.53%, whereas MnO wt% from 0.06 to 0.20%. The concentration of TiO_2 wt% ranges from 0.48 to 1.68%.

The bivariate diagram (Fig. 6) of appropriate major oxides plot of SiO_2 versus Fe_2O + MgO + MnO concentration exhibits moderate enrichment of ferromagnesian elements with linear negative correlation suggesting that these are the product of fractional crystallization from the parental magma. In contrast, there is a broad, but strong positive correlation between SiO_2 and total alkalies (Na_2O + K_2O) indicating progressive fractionation of mafic melt. The LILE elements like Sr/Rb ratio exhibits an apparent declination with increasing SiO_2 reflecting the relative fractionation of both plagioclase and K-feldspar. The abundance of HFSE such as Zr/Y ratio exhibits a relatively coherent negative trend with increasing SiO_2. Most of the amphibolites have less enrichment of MgO content with a slightly positive correlation of Cr (compatible element). However, the concentration of MgO is less than 07 wt% with low Ni values below 200 ppm and lower Mg# (~0.34) advocates the fractionation of MgO rich phases.

Geochemical classification using total alkalis versus silica (TAS) diagram of Le bas et al. (1979) shows that the amphibolites are predominantly basalt to basaltic-andesite composition (Fig. 7a), whereas the high field strength elements such as Nb/Y vs Zr/Ti ratio plot (modified by Pearce, 1996) exhibits basaltic composition (Fig. 7b). For magma characterization, the amphibolites classified as tholeiitic magmatic series on the bivariate plot of FeO^t/MgO vs. SiO2 (Miyashiro, 1974) with the exception of three samples distinguishes as calc-alkaline series (Fig. 7c). The tholeiitic and calc-alkaline series can be differentiated in terms of their trends on an AFM diagram (Irvin and Baragar, 1971), in which amphibolites follow the tholeiitic series trend indicate strong enrichment of iron in the early stages of differentiation (Fig. 7d). Further, the amphibolites are characterized into high-Fe tholeiite basalt on the ternary plot (Al, Mg and Fe^T + Ti) of Jensen, 1976 (Fig. 7e).

In the tectonic discrimination diagram of Th - Zr/117 - Nb/16 for most of the samples clearly shows volcanic arc basalt character (Fig. 7f). From the tectonic plot of Zr-Zr/Y (Pearce and Norry, 1979) most of the amphibolites are classified as island arc basalts (Fig. 8a). However, the MgO - Fe_2O_3 - Al_2O_3 ternary diagram of Pearce et al. (1977) reflects variable discrimination but the majority of the metavolcanic rock samples from the study area indicate their ocean island affinity (Fig. 8b).

Table 1: Major and Trace concentrations for the amphibolites from Khammam schist belt, eastern margin of EDC.

Sample No.	SV-55	SV-59	SV-61	SV-104	SV-44A	SV-72	SV-91	SV-159	SV-161	SV-162
Oxides (wt %)										
SiO_2	49.16	50.15	50.75	49.51	52.06	49.80	51.78	47.76	50.60	51.07
Al_2O_3	10.54	12.15	11.48	6.25	12.31	13.78	11.09	10.53	11.04	10.57
Fe_2O_3	14.97	11.05	13.53	10.63	8.36	14.18	15.12	16.77	14.07	14.22
MnO	0.18	0.16	0.16	0.20	0.06	0.15	0.13	0.20	0.15	0.14
MgO	6.61	9.50	6.58	12.60	8.80	4.64	4.87	5.92	6.64	6.46
CaO	9.97	10.67	9.89	13.21	10.25	10.48	9.75	10.51	10.67	10.46
Na_2O	1.63	1.67	2.43	1.01	3.53	2.21	1.51	1.60	1.73	1.88
K_2O	0.36	0.54	0.31	0.50	0.65	0.57	1.67	0.56	0.41	0.31
TiO_2	1.68	0.87	1.42	0.48	1.04	1.29	0.68	1.50	0.70	0.84
P_2O_5	0.19	0.18	0.25	0.14	0.53	0.18	0.13	0.27	0.12	0.16
Mg#	0.31	0.46	0.33	0.54	0.51	0.25	0.24	0.26	0.32	0.31
Trace (ppm)										

Ba	168.53	280.83	579.30	740.78	140.82	122.49	242.15	205.46	259.58	110.94
Ga	20.14	12.01	17.47	10.92	17.67	17.51	12.68	17.54	14.06	13.96
Sc	44.32	36.54	45.26	41.32	22.68	48.35	49.55	47.36	51.98	50.51
V	346.09	242.20	296.09	187.36	187.36	406.38	272.83	406.95	334.05	332.27
Th	2.00	4.47	2.00	2.00	2.00	4.42	2.00	2.00	2.00	2.00
Pb	1.79	7.53	2.13	9.58	7.98	4.88	3.50	3.05	0.80	4.88
Ni	45.92	198.40	37.71	83.41	144.18	68.16	86.41	75.79	85.96	87.15
Co	41.39	46.16	44.85	48.82	20.45	56.86	49.27	56.79	61.15	58.60
Rb	2.50	10.48	2.50	11.96	2.50	22.92	43.19	11.27	13.27	9.34
Sr	159.54	206.85	380.76	194.55	279.85	108.86	108.02	105.09	86.18	86.27
Y	36.17	26.55	29.14	35.64	46.25	32.99	30.55	38.96	19.58	23.46
Zr	119.03	81.13	75.72	61.00	409.17	82.07	40.49	84.17	29.12	37.97
Nb	7.29	5.55	6.96	2.50	14.80	5.39	2.50	5.89	2.50	2.50
Cr	137.63	698.64	70.85	421.58	334.72	108.20	152.53	119.17	128.86	125.59
Cu	21.65	145.58	94.65	104.49	3.16	182.99	120.86	230.73	214.95	226.19
Zn	91.26	87.78	73.92	99.96	29.72	83.34	41.31	96.94	81.78	82.89
Sr/Rb	63.82	19.74	152.30	16.27	111.94	4.75	2.50	9.32	6.49	9.24
Zr/Y	3.29	3.06	2.60	1.71	8.85	2.49	1.33	2.16	1.49	1.62
Ba/Nb	8.55	18.71	30.78	109.59	3.52	8.40	35.82	12.90	38.40	16.41
La/Nb	5.35	3.04	1.87	16.26	7.50	2.08	3.29	6.14	2.99	4.97
Th/Nb	5.33	15.64	5.58	15.53	2.62	15.92	15.53	6.59	15.53	15.53
Nb/Yb	2.73	2.62	2.91	1.08	3.95	2.04	0.83	1.77	1.47	1.24

Table 2: Concentrations of REEs in amphibolites from Khammam schist belt, eastern margin of EDC.

Sample No.	**SV-55**	**SV-59**	**SV-61**	**SV-104**	**SV-44A**	**SV-72**	**SV-91**	**SV-159**	**SV-161**	**SV-162**
REEs (ppm)										
La	41.87	18.11	13.94	43.61	119.04	12.01	8.82	38.80	8.03	13.34
Ce	88.63	35.88	30.18	116.24	282.97	26.37	17.64	89.81	15.41	30.34
Pr	11.28	4.37	3.80	15.93	27.78	3.29	2.11	10.35	1.87	3.92
Nd	46.87	17.92	16.86	70.24	108.11	14.44	9.09	42.77	7.95	16.46
Eu	2.54	1.44	1.51	2.52	4.38	1.24	0.98	2.49	0.70	1.20
Sm	9.07	4.31	4.23	14.47	17.68	3.84	2.49	8.04	2.04	3.76
Tb	1.36	0.85	0.94	1.78	1.98	0.91	0.76	1.34	0.49	0.74
Gd	8.07	4.90	5.36	11.75	14.19	5.01	3.60	7.98	2.80	4.27
Dy	7.91	5.25	5.88	8.29	10.33	6.15	5.19	8.22	3.20	4.49
Ho	1.42	1.00	1.12	1.39	1.82	1.20	1.14	1.62	0.73	0.86
Er	3.88	2.81	3.24	3.59	5.27	3.73	4.02	4.88	2.17	2.76
Tm	0.62	0.40	0.54	0.55	0.72	0.55	0.60	0.74	0.30	0.44
Yb	3.49	2.78	3.13	3.02	4.91	3.47	3.93	4.36	2.22	2.63
Lu	0.57	0.40	0.54	0.48	0.73	0.56	0.72	0.70	0.38	0.45
LaN/YbN	8.09	4.40	3.01	9.73	16.35	2.34	1.51	6.01	2.44	3.42
EuN/YbN	2.07	1.47	1.38	2.37	2.53	1.02	0.71	1.62	0.89	1.29
Eu/Eu*	0.91	0.96	0.97	0.59	0.84	0.86	1.00	0.95	0.89	0.91
∑ REE	**227.58**	**100.41**	**91.28**	**293.88**	**599.90**	**82.77**	**61.07**	**222.09**	**48.28**	**85.68**

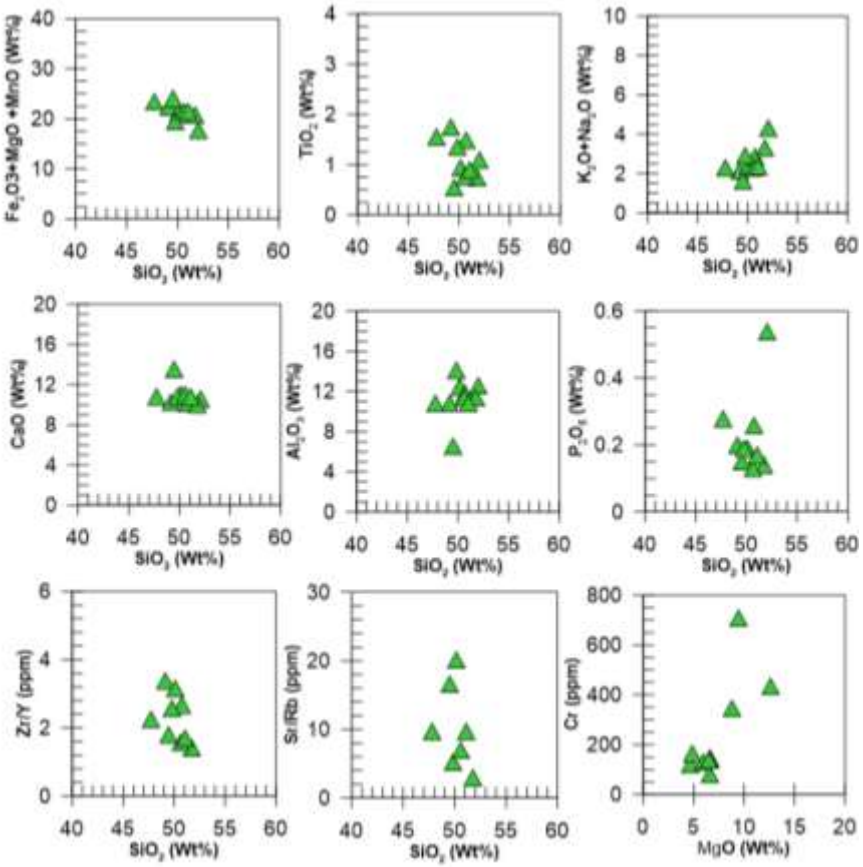

Figure. 6 Bivariate plots of major oxides and trace elements showing the significant correlation trends for the amphibolites.

The abundance of trace elements, HFSE and REE provide a detailed picture of geochemical significance. The amphibolites of the area consist of relatively low TiO_2 (~1.00 ppm), Cr (~229.77 ppm), Nb (~5.58 ppm), Th (2.48 ppm) and Y (~31.92 ppm). From the primitive mantle normalized REE spider plot (Sun & McDonough 1989) it is clear evidence that the amphibolites of the area are characteristics of island arc basalts (IAB) considerably showing more enrichment of LILE such as Rb, Sr and Pb, with depletion in HFSE such as Nb and Ti and LREE relative to neighbouring elements and less enrichment in heavy rare earth elements (Fig. 8c). Compared with the normalized profiles of normal-MORB (Sun & McDonough 1989) most of the samples have strong enrichment of large ion lithophile elements (LILE) like Th with variable low enrichment of high field strength elements (HFSE) like Nb, Ti and light rare earth elements (LREE) anomalies (Fig. 8d) suggest that, the parent magma were considerably contaminated with crustal material. Further, they are also characterised by high $(Ba/Nb)_N$ = 28.30, $(La/Nb)_N$ = 5.34 and low $(Th/Nb)_N$ = 11.38, $Nb/Yb)_N$ = 2.06 ratios indicating low partial melting of mantle and relatively higher subduction input during the evolution of magma. However, pronounced negative troughs of Nb and Ti can arise from the remelting of arc crust (Whalen et al., 1998; Morris et al., 2000) and/or from the fractionation of HFSE- and Ti-enriched phases (Green and Pearson, 1987; Ryerson and Watson, 1987; Lentz, 1999). On the Chondrite normalized REE diagram (Sun and McDonough, 1989), the less number of amphibolites samples show slightly LREE enrichment (La/Sm_N = 1.89 to 4.23) with nominal fractionation trend, but flat HREE pattern and insignificant Eu anomaly (Eu/Eu* = ~ 0.88) indicates nominal fractionation of plagioclase (Fig. 8e).

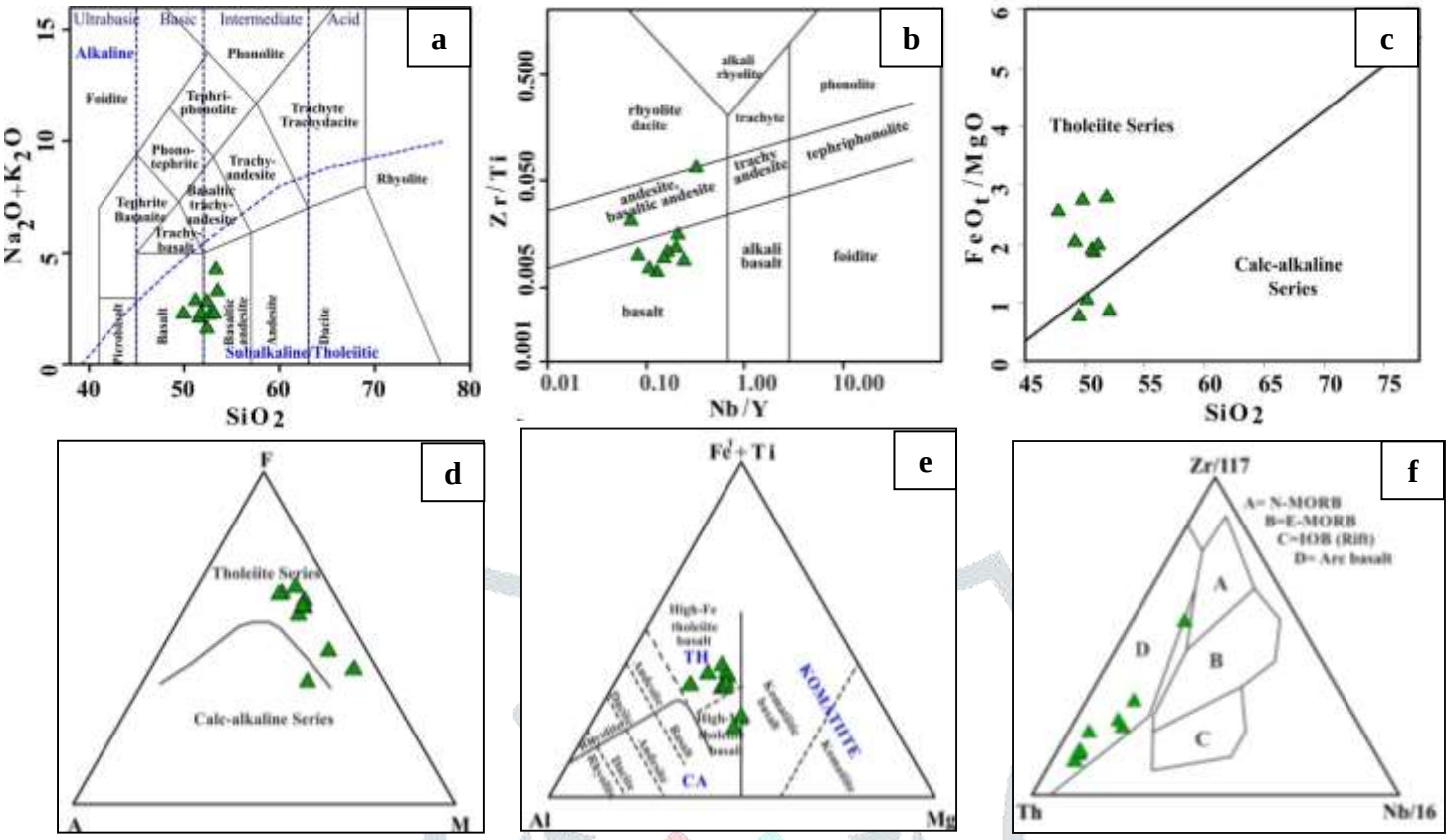

Figure 7 (a) Chemical classification scheme SiO_2 vs. $Na_2O + K_2O$ diagram (after Le Bas et al., 1986) of the amphibolites. (b) Nb/Y vs. Zr/Ti ratio diagram (Winchester & Floyd, 1977, modified by Pearce, 1996). c) SiO_2 vs FeO^T/MgO plot showing the Tholeiitic nature of the magma series of amphibolites. d) The AFM diagram (fields by Irvine and Baragar, 1974) showing magmatic series trend of amphibolites. e) Ternary diagram of Al, Mg and Fe^T + Ti diagram showing magmatic High-Fe tholeiitic character (Jensen, 1976). (f) The plot of Th - Zr/117 - Nb/16 on ternary diagram (Wood et al., 1980) for amphibolites classified as Arc basalt.

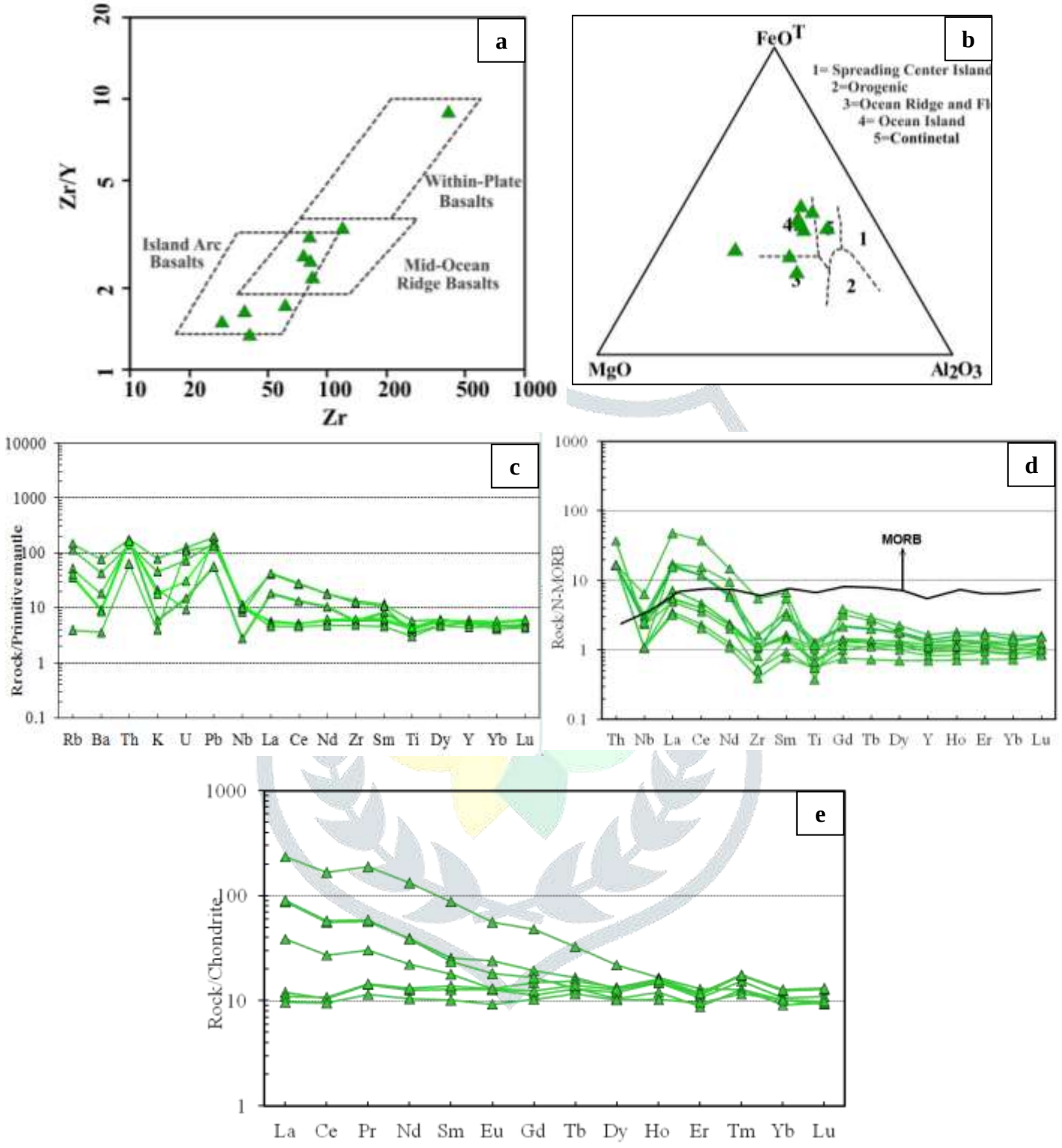

Figure 8(a). Tectonic discrimination diagram of Zr vs Zr/Y (Pearce and Norry, 1979) for the amphibolites are mostly confining into Island Arc Basalt. (b) The MgO-Fe_2O_3-Al_2O_3 ternary diagram of Pearce et al., (1977) showing amphibolites clustered as Oceanic Island. (c) Geochemical behavior of LILE and REEs for the amphibolites on multi-element diagram (primitive mantle normalizing values after Sun & McDonough, 1989). (d) N-MORB (normal mid oceanic ridge basalt) diagram showing the HFSE and REEs pattern of the amphibolites (normalizing values after Sun & McDonough, 1989). (e) Chondrite normalized diagram (normalizing values after Sun and McDonough, 1989) showing the REE pattern of metabasalt.

6. DISCUSION AND CONCLUSION:

Unlike other schist belts of Telangana, the amphibolites of the Khammam schist belt do not form continuous bands in the area. They only occur as small sporadic enclaves within the country-rock of granite gneisses of PGC-II. However, these enclaves follow the regional foliation pattern parallel to the gneissic foliation of granite gneisses. The contrary, amphibolites of the Khammam schist belt in proximity to the Chimalpahad anorthosite complex have been examined by various authors both petrographically as well as geochemically. But, the area under their investigation is a complex terrane that witnessed strong multiple deformations as well as metamorphism having a large volume of intrusives activity. Therefore, the amphibolites near Chimalpahad and the surrounding zone may give erratic geochemical signatures. Though the geochemical signatures are similar for amphibolite from the Chimalpahad area, the field characteristics and mutual relationship with surrounding country-rock are completely different for amphibolite from the south of Wyra. The comparative field observations and their silent features of the amphibolites from different areas are mentioned in Table 3. Comparatively, the present study area is a suitable location where the rocks of the Khammam schist belt do not have a direct influence of much basic intrusive activity. Based on field relationship, the amphibolites of the area characterised in detailed megascopically as well as petrographically and different geochemical classification schemes were presented to know the magmatic evolution of the Khammam schist belt. Though the amphibolites of the Khammam schist belt witnesses the epidote-amphibolite facies metamorphism geochemically they constitute moderate SiO_2 (<52 wt %), Al_2O_3 (<10.81 wt %), Fe_2O_3 (~13.16 wt %) with low Mg# ~0.36 wt % and TiO_2 (<1.0 wt %) concentrations indicating amphibolites of the area still retains its basic magmatic signatures along the eastern margin of the EDC. Most of the amphibolite samples show basaltic to basaltic-andesite composition and distinguished into tholeiitic magma series. Geochemical signature reveals that the amphibolites of the area contain relative enrichment in large ion lithophile elements (LILE) Rb, Th, K and Pb and light rare earth elements (LREE) with less enrichment in heavy rare earth elements (HREE), but depletion in high field strength elements (HFSE), such as Nb and Ti shows the characteristics of Island Arc Basalts (IAB).

Table 3: General characteristic features and field correlation for amphibolite of KSB form various areas.

Amphibolite from Chimalpahad Complex	Amphibolite from south of Wyra
Predominantly garnetiferous, strongly deformed and highly metamorphosed with development of felsic leucosome (melt)	Majority are non-garnetiferous occasionally garnetiferous confined to massive variant and comparatively weakly metamorphosed without leucosome
Numerous intrusive activity effect of gabbro-anorthosite and gabbro-dolerite associated with amphibolites	Devoid of basic intrusive activity and all amphibolite bands occurs as enclaves within the granite gneiss
Supracrustal amphibolite and amphibolite dykes confined to one single metamorphic regime of almandine - amphibolite facies	Mineral assemblages suggests epidote-amphibolite facies of metamorphism

ACKNOWLEDGMENT

A deep sense of gratitude is also accorded to the Director General, GSI, CHQ, Kolkata, for providing all the necessary facilities. Sincere thanks extended towards the Head of the Department, Geological Survey of India, Sothern Region, Hyderabad, for providing all the necessary laboratory facilities and proper execution of the work. My deepest appreciation is expressed to Dr. Abhijit Roy, Director, Dr. Subrata Chakraborty, DyDG, SU: Telangana, SR, GSI, Hyderabad, and Dr. Vikash Tripathy, Sr. Geologist, SR, GSI, Hyderabad, who gave technical guidance, immense support and valuable suggestions for improving the manuscript. The authors express a sincere thanks to the Head of the Department, Applied Geology, for encouraging the research work. Special thanks to Syed Muzimuddin, GSI, Hyderabad, for improving various maps.

REFERENCES:

Ajit Kumar Reddy, T. 1976. Geology of parts of Khammam and Madhira taluks, Khammam district, A.P. Unpub. Rep. GSl for the FS 1975 - 76.

Appavadhanulu, K. 1961. Geology of parts of Chimalpahad hill range in Khammam district, Andhra Pradesh. Progress report for field season, 1960-61 of GSI.

Appavadhanulu, K., Setti, D.N., Badrinarayanan, S. and Subba Raju, M. 1976. The Chimalpahad meta-anorthosite complex, Khammam district, Andhra Pradesh. Geology Survey of India, Miscellaneous Publication, 23: 267–278.

Babu, V.R.R.M. 1998. The Nellore schist belt: an Archean greenstone belt, Andhra Pradesh, India. Gondwana Res. Gr. Mem., 4: 97-136.

Hari Prasad et al. 2000. Petrology and geochemistry of amphibolites from the Nellore-Khammam schist belt, SE India. Journal of the Geological Society of India 56 (1): 67-78.

Irvin, T. N. and Baragar, W. R. A. 1971. A guide to chemical classification of the common volcanic rocks. Can . J. Earth. Sci., 8: 523—548.

Leelanandam, C. and Narsimha Reddy M. 1985. Petrology of the Chimalpahad anorthosite complex, Andhra Pradesh, India. News Jahrbuch Mimer. Abh., Vol., 153: 91-119.

McDonough W. F., and Sun S. S. 1995. The composition of the Earth; Chem. Geol., 120: 223–253.

Miyashiro, A. 1970. Volcanic rock series in island arcs and active continental margins. American Journal of Science, 274: 321–355.

Miyashiro, A. 1970. Volcanic rock series in island arcs and active continental margins. American Journal of Science, 274: 321–355.

Moeen, S. 1998. P-T estimates from Nellore schist belt (India) and evidence for superimposed metamorphic event. Ceol. Jour., 33: 1-15.

Okudaira et al. 2001. Sm-Nd and Rb-Sr dating of amphibolite from the Nellore-Khammam schist belt, SE India: Constraints on the collision of the Eastern Ghats terrane and Dharwar-Bastar craton. Geol. Mag., 138 (4), 2001: 495–498.

Pearce J. A., Harris N. B., W and Tindle A. G. 1984. Trace element discrimination diagrams for the tectonic interpretation of granitic rocks; J. Petrol., 25: 956–983.

Ramam, P.K. and Murty, V.M. 1997: Geology of Andhra Pradesh. Geological Society of India, Bangalore, 245.

Sarvothaman, H. 1995. a) Geology of Khammam schist belt and its environs, Andhra Pradesh. Rec. Geol. Surv. India, 128: 38-40.

Sarvothaman, H. 1995. b) Amphibolites of Khammam chist belt: evidence for the Precambrian Fe-tholeiitic volcanism in marginal zone. Indian Mineral., 49: 177- 186.

Srihari, J. Basha, S.M.J., Charyulu, D.N. and Narahari, S.T. 2004. Report on the Specialised Thematic Mapping of Shernawala Tectonic Zone in the parts of Krishna and Khammam Districts, Andhra Pradesh. Progress report of GSI.

Srinivasan, K. N. and Gaensan, V. 1986. Geology of parts of Khammam district, Andhra Pradesh. Progress report of GSI.

Subbaraju, M. 1975. Some aspects of the schistose rocks of Khammam district, Andhra Pradesh. Indian Mineralogist, 16: 35-42.